

The New Multi-Frequency ECRH System for ASDEX Upgrade

WAGNER Dietmar¹⁾, LEUTERER Fritz¹⁾, MANINI Adriano¹⁾, MONACO Francesco¹⁾, MÜNICH Max¹⁾,
RYTER François¹⁾, SCHÜTZ Harald¹⁾, STOBER Jörg¹⁾, ZOHN Hartmut¹⁾, FRANKE Thomas¹⁾,
DANILOV Igor²⁾, HEIDINGER Roland²⁾, THUMM Manfred³⁾, GANTENBEIN Gerd³⁾,
KASPAREK Walter⁴⁾, LECHTE Carsten⁴⁾, LITVAK Alexander⁵⁾, DENISOV Gregory⁵⁾, TAI Evgeny⁶⁾,
POPOV Leonid⁶⁾, NICHIPORENKO Vadim⁶⁾, MYASNIKOV Vadim⁶⁾, SOLYANOVA Elena⁶⁾,
MALYGIN Sergey⁶⁾, MEO Fernando⁷⁾, WOSKOV Paul⁸⁾

¹⁾Max-Planck-Institut für Plasmaphysik, EURATOM-IPP, Boltzmannstr.2, D-85748 Garching, Germany

Forschungszentrum Karlsruhe, Association Euratom-FZK, ²⁾Institut für Materialforschung,

³⁾Institut für Hochleistungsimpuls- und Mikrowellentechnik, D-76021 Karlsruhe, Germany

⁴⁾Institut für Plasmaforschung, Universität Stuttgart, D-70569 Stuttgart, Germany

⁵⁾Institute of Applied Physics, 46 Ulyanov St., Nizhny Novgorod, 603950, Russia

⁶⁾GYCOM Ltd, 46 Ulyanov St., Nizhny Novgorod, 603155, Russia

⁷⁾Association EURATOM-Risø National Laboratory, DK-4000 Roskilde, Denmark

⁸⁾MIT Plasma Science and Fusion Center, Cambridge, MA 02139, USA

Abstract

A new multi-frequency ECRH system is currently under construction at the ASDEX Upgrade Tokamak experiment. This system will, for the first time in a fusion device, employ multi-frequency gyrotrons, step-tunable in the range 105-140 GHz. In its final stage the system will consist of 4 gyrotrons with a total power of up to 4 MW and a pulse length of 10 s. The variable frequency will significantly extend the operating range of the ECRH system both for heating and current drive. The Matching Optics Unit (MOU) includes a set of phase correcting mirrors for each frequency as well as a pair of broadband polarizer mirrors. The transmission line consists of nonevacuated corrugated HE₁₁ waveguides with I.D. = 87 mm and has a total length of about 70 m. A fast steerable launcher enables the steering of the beam over the whole plasma cross section poloidally. The first two-frequency gyrotron has been installed recently. It is equipped with a single-disc diamond window. The next gyrotrons will be step-tunable with two additional frequencies between 105 and 140 GHz. They will require a broadband output window which will be either a Brewster or a double-disc window.

1. Introduction

The power deposition in the plasma is primarily determined by the magnetic field $B(r)$. For a single frequency ECRH system this has the consequence that for central heating the magnetic field is no longer a free parameter. However, for plasmas with different plasma currents or different equilibria, the magnetic field should be a free parameter in order to operate at a reasonable edge safety factor $q(a)$. Furthermore, in a plasma with given parameters, some experimental features, like suppression of neoclassical tearing modes (NTM), require to drive current on the high field side without changing the magnetic field. These requests can be satisfied if the gyrotron frequency is variable ¹. In the experiments performed up to now in ASDEX Upgrade, the installed power was only 2 MW, of which 1.6 MW was coupled to the plasma. This imposes a limit for current drive, NTM stabilization or generation of internal transport barriers ². The requirement for the new system is therefore an installed power of 4 MW. Since the current diffusion time in hot plasmas, like those with an internal transport barrier and $T_e > 10$ keV, is several seconds, we need a pulse duration of 10 s compatible with the limit of ASDEX Upgrade flat top discharges. A further requirement is the capability for very localized power deposition such that its center can be feedback controlled, for instance to keep it on a resonant q -surface. For this purpose fast movable mirrors have been installed.

The paper describes the main components of the new system (gyrotrons, MOU, transmission line, vacuum windows and launcher) with its peculiarities that are mainly connected to the application of multiple frequencies.

2. Gyrotrons

Step-tunable gyrotrons oscillate for each frequency in a different cavity mode. Fig. 1 shows an example of possible modes and frequencies. Short pulse test gyrotrons have demonstrated efficient generation of power in excess of 1 MW at all these frequencies ^{4,5}. The first two-frequency GYCOM gyrotron Odyssey-1 (Fig. 2) has been installed and put into operation. It can work at 105 GHz and at 140 GHz. The corresponding operating modes are $TE_{17,6}$ and $TE_{22,8}$. Here we make use of the $3\lambda/2$ and $4\lambda/2$ resonances (λ is the wavelength) of the single-disc synthetic diamond vacuum window at these frequencies. The gyrotron has a single-stage depressed collector. Therefore the cathode voltage can be limited to a maximum value of 60 kV. The maximum beam current is 40 A. There is a separate set of series tetrode and body modulator for each gyrotron (Fig. 3), which will allow maximum flexibility for the experimental program. The frequency can be changed between two ASDEX Upgrade pulses and requires an adjustment of the cryomagnetic field, the gun and collector magnetic fields and operating voltages. Reliable operation was achieved, only limited by the available high power long-pulse load. The measured output power at 105 GHz and 140 GHz was 610 kW and 820 kW, respectively for a pulse length of 10 s. For NTM stabilization experiments a fast modulation capability of the gyrotrons is required. This is especially important for future experiments like ITER where the width of the driven EC current will be larger than the marginal island size of the NTM leading to a loss of current drive efficiency in the non-modulated case ⁶. Two modulation schemes have been tested with this gyrotron. A 100% power modulation up to 0.5 kHz was achieved by switching both, cathode and body voltage on and off. This scheme will be mainly used for heat wave analysis. Higher modulation frequencies up to 25 kHz with modulation depths up to 90 % were achieved by a reduction of only the cathode voltage from 42 kV to 25 kV while keeping the body voltage constant. First plasma test shots were performed with a maximum power of 820 kW at 140 GHz and a pulse length up to 0.8 s. The total measured frequency variation during a gyrotron pulse was 140 MHz ⁷. Out of this, a drift of ~ 100 MHz happens in the first 100 ms of the pulse and repeatedly during on/off modulation (Fig. 4), very likely due to space charge effects and

plasma formation in the cavity⁸. The remaining shift of 40 MHz to steady state results from the thermal expansion of the cavity.

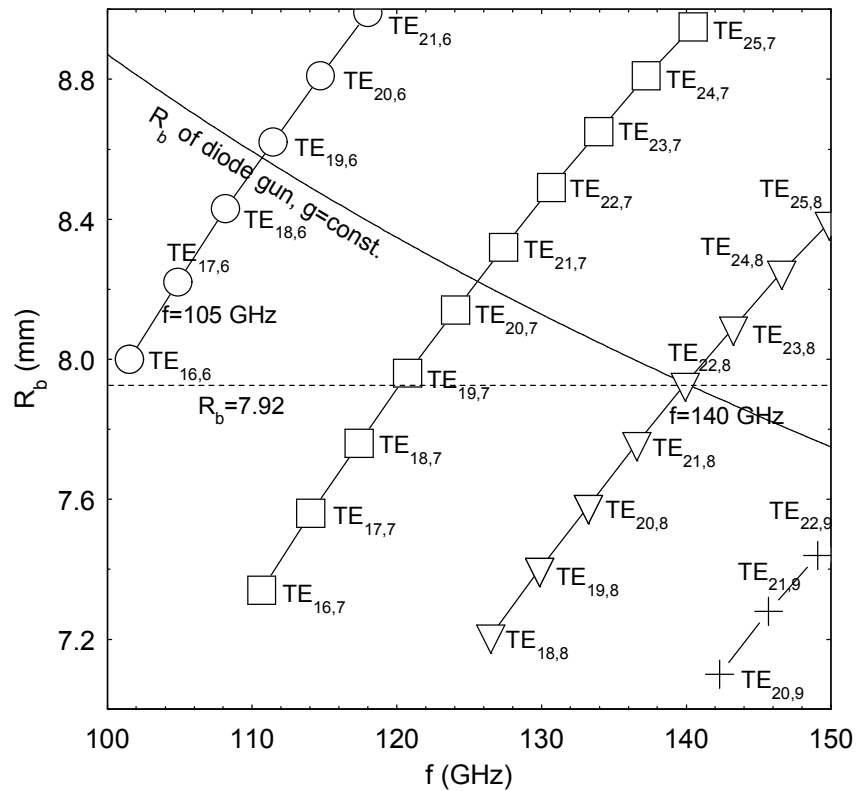


Fig. 1 Electron beam radii and frequencies for operating $TE_{m,n}$ modes of the step-tunable gyrotron. Also shown are curves for constant beam radius ($R_b = 7.93$ mm) and R_b as a function of frequency for constant pitch factor ($g = \text{const.}$).

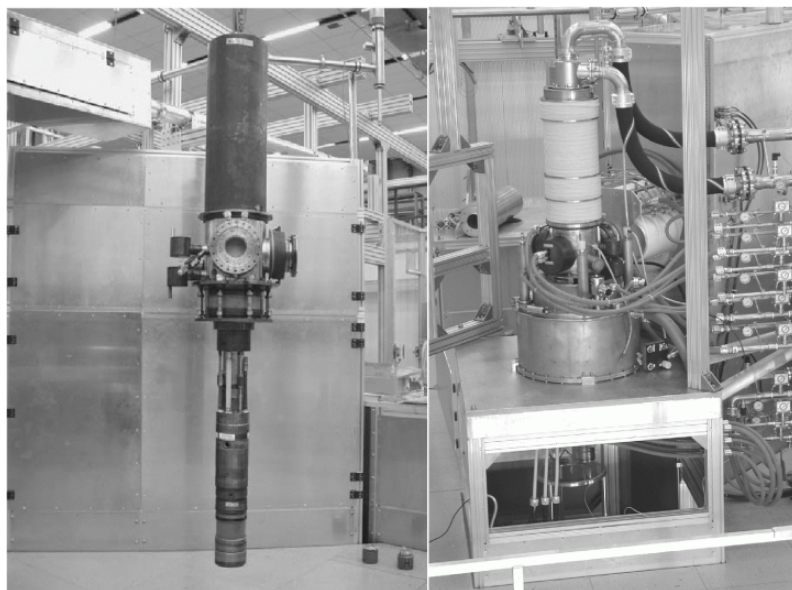


Fig. 2 Two-frequency gyrotron Odyssey-1 (GYCOM) before (left) and after installation in the magnet (right).

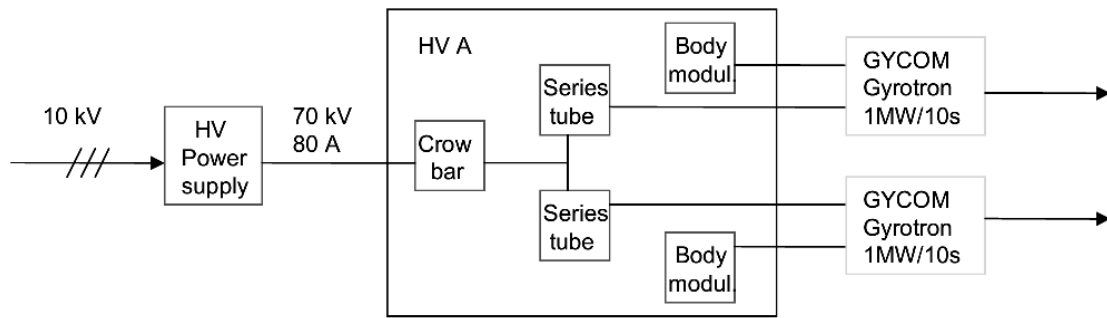


Fig. 3 Schematic of power supply and modulator setup.

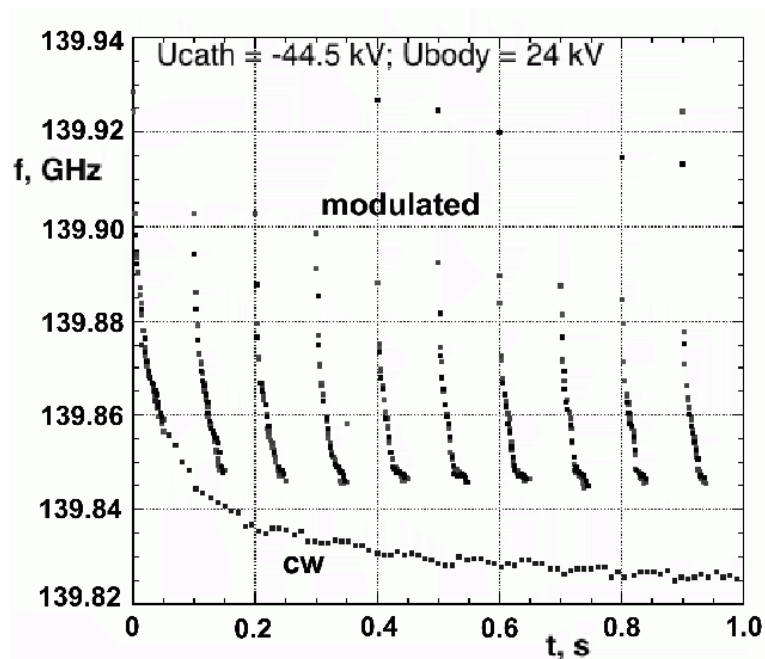


Fig. 4 Measured frequency drift of gyrotron Odyssey-1 during a modulated (50ms/50ms) and a cw 140 GHz pulse.

3. Matching Optics Unit and Transmission Line

One of the complicating features with step-tunable gyrotrons is that the output beam leaves the gyrotron window at slightly different azimuthal angles and positions due to the varying caustic radii for different modes (Fig. 1). Therefore the MOU (Fig. 5) contains different sets of phase correcting mirrors (M1, M2) to match the gyrotron output beam at different frequencies to the transmission line input. In order to limit the number of required phase correcting mirror sets we chose four frequencies as our main operating modes for the step-tunable gyrotrons. The phase correcting mirrors are mounted on rotating discs and can be set according to the operating frequency. The second mirror M2 contains a coupling-hole array for pulse monitoring and power measurement. Only one set of polarizers (P1, P2) with groove depths of $\lambda/4$ and $\lambda/8$ scaled to the center frequency of 122.5 GHz proved to be sufficiently broadband to provide the required range of ellipticity and orientation of the polarization ellipse for all necessary injection angles over the whole frequency band of the system (105-140 GHz)⁹. Figure 6 shows the calculated polarization ellipticity of the output beam of the

launcher in dependence of the polarizer angles for three different frequencies. The figure includes the polarizer angles (indicated by markers) for the most critical launching conditions, where the low frequency limit first occurs. Each marker represents a combination of polarizer angles that provide efficient coupling ($> 99\%$) to the x-mode in the plasma. The almost linear polarization required for central heating (poloidal and toroidal angles of 10° and 0° respectively) is the first solution that vanishes outside of the frequency band of the two-polarizer system⁹. The MOU contains also two switching mirrors that can direct the beam to a 1 s calorimetric load which is part of each MOU, or to a central long pulse load. Using the 1 s loads, all four gyrotrons can be started up simultaneously every day. Fig. 7 shows the gyrotron setup with a MOU connected to each gyrotron. The transmission to the torus is in normal air, through corrugated aluminum HE_{11} waveguides with I.D.= 87 mm over a total length of about 70 m. Since most part of the waveguide path is straight, the number of miter bends could be limited to eight. Another calorimetric load (0.1 s) is installed at the end of the transmission line at the torus. This load is used to test the transmission line prior to plasma shots as well as for calorimetric measurements of the transmission efficiency. The measured transmission loss is 12 % at 105 GHz and 10 % at 140 GHz, which is in reasonable agreement with the theoretical predictions (Table 1). The higher measured loss is due to limited mode purity both of the free-space gyrotron output beam as well as the excited HE_{11} mode in the waveguide. Spill-over losses at the MOU mirrors, which are not included in the estimation, are also expected to increase at lower frequencies due to higher beam divergence.

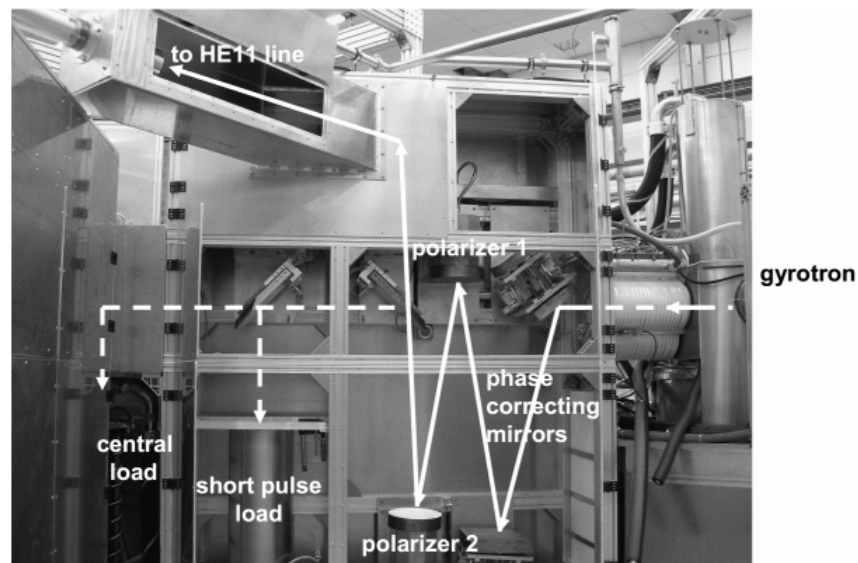


Fig. 5 Matching optics unit with phase correcting mirrors and polarizers.

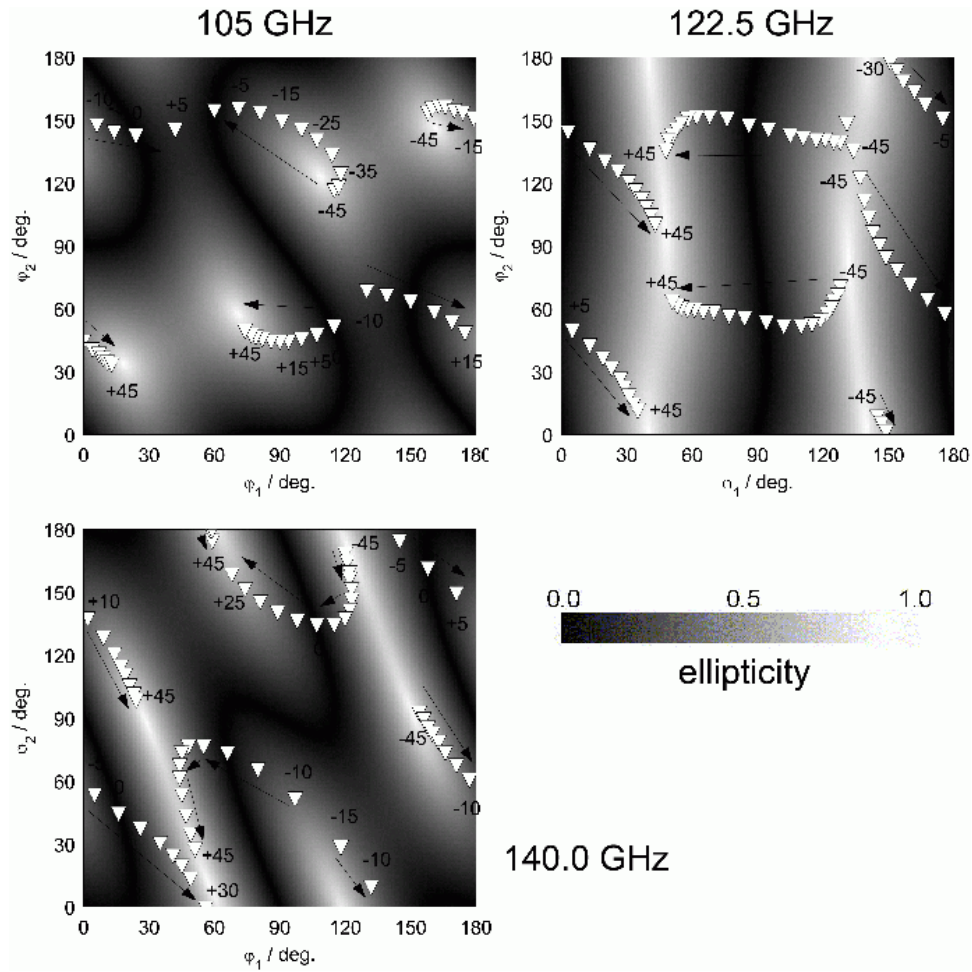


Fig. 6 Calculated ellipticity of the broadband two-polarizer set. Indicated by the markers are the required ellipticities for a toroidal angular sweep at a constant poloidal angle of 10° ($B_t = 2.4$ T, $I_p = 800$ kA).

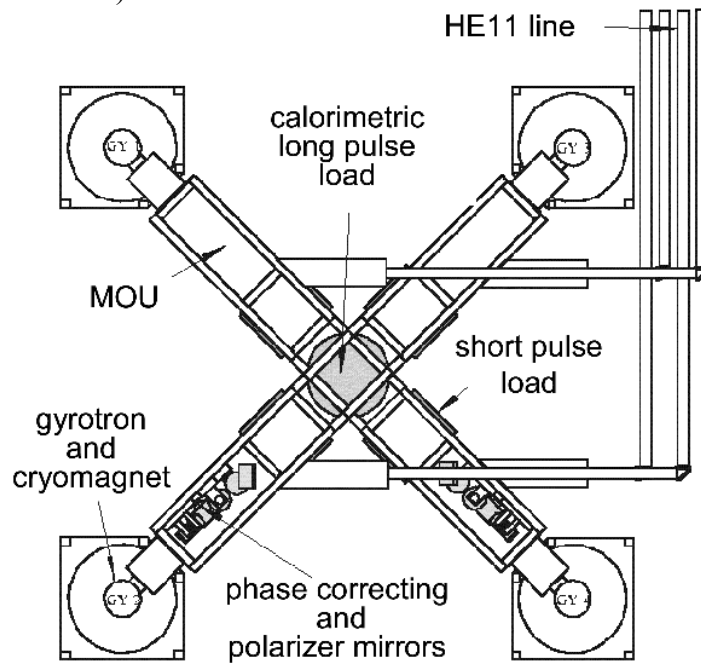


Fig. 7 Gyrotron setup with four matching optics units and central long pulse load.

Frequency	105 GHz	140 GHz
Ohmic loss (70m HE ₁₁ waveguide)	0.12%	0.05%
Ohmic loss (8 miter bend mirrors)	0.76	1.03
Diffraction loss (8 miter bends)	5.28	3.43
Atmospheric absorption (L=70m)	1.2%	3.17
Total estimated loss	7.36%	7.68%
Measured loss	12%	10%

Table 1 Estimated and measured loss of the HE₁₁ waveguide transmission line.

4. Broadband Vacuum Window

Except for the two-frequency gyrotron, where a single-disc diamond window is transparent at both frequencies, the vacuum windows required for the step-tunable gyrotron and at the torus must be broadband. For the gyrotron with its linearly polarized output beam two options for a broadband output window exist, a Brewster window or a tunable double-disc window. Fig. 8 shows the concept of both windows. The gyrotron with Brewster window requires additional mirrors providing the passing of the beam through the window at the correct angle (Fig. 8a). To avoid constraints with respect to polarization which is set by the two polarizers in the MOU, a tunable double-disc window with a remote controlled adjustment of the distance between the discs will be used at the torus (Fig. 8b). Two diamond discs with a thickness of 1.8 mm will be utilized for this window, where the discs themselves are resonant at 105 and 140 GHz ($3\lambda/2$ and $4\lambda/2$ respectively). For intermediate frequencies the double-disc window can be tuned to a reflection minimum by changing the distance between the two discs. A mounted double-disc window for the ASDEX Upgrade torus is shown in Fig.9. Fig. 10 plots the calculated reflection for different distances between the discs. A critical value is the width of the Fabry-Perot resonances at intermediate frequencies between the single-disc resonances. Only a maximum distance of 10 mm between the discs can be allowed for a possible frequency drift of 140 MHz during the gyrotron pulse to keep the reflection below the critical value of 1 %. The volume between the two discs will be evacuated in order to increase the power handling capability.

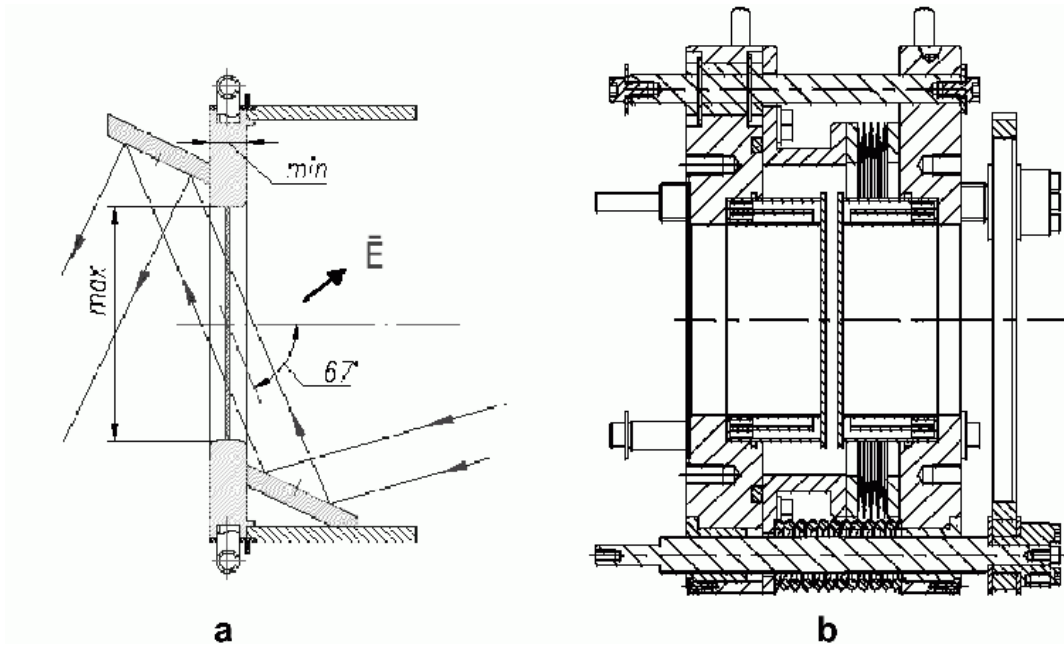


Fig. 8 Schematic of both broadband windows: (a) Brewster and (b) double-disc.

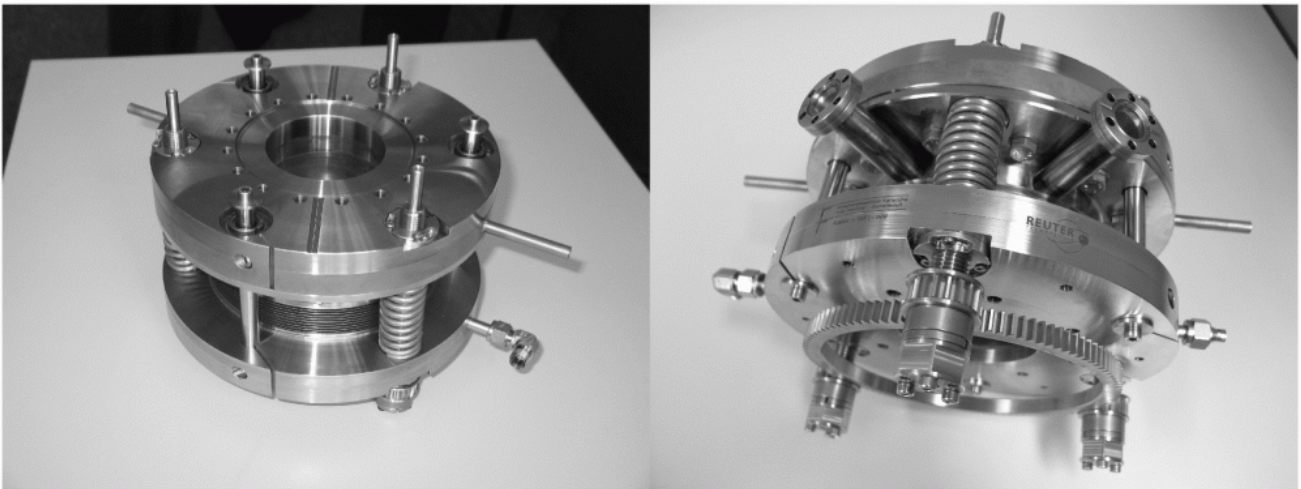


Fig. 9 Broadband double-disc torus window for ASDEX Upgrade.

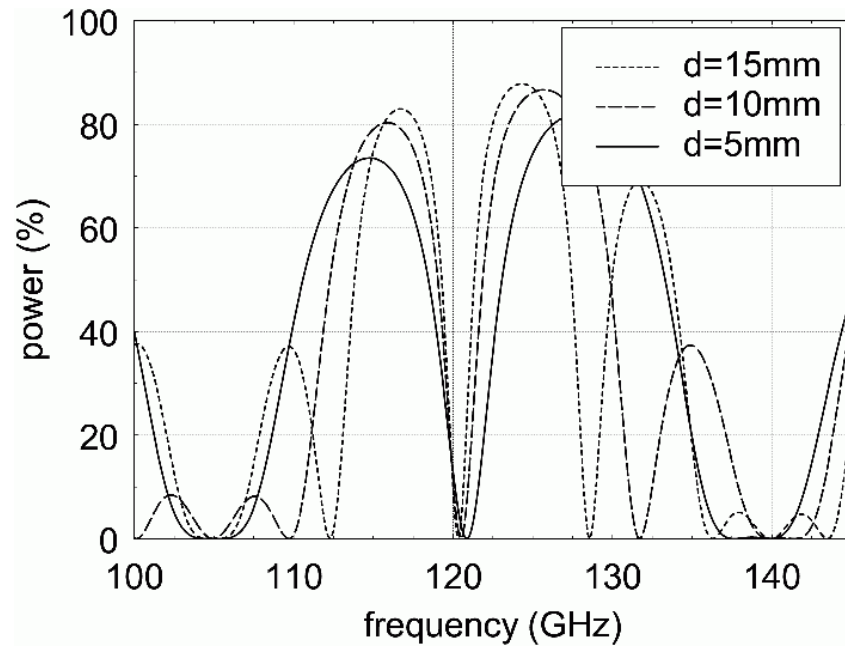


Fig. 10 Calculated reflection of a double disc window for different distances d between the discs.

5. Fast Steerable Launcher

A steerable launcher (Fig. 11) will enable the steering of the beam over the whole plasma cross-section. In order to cope with thermal load, disruption forces and mechanical dynamics of the fast poloidal steering, the mirror is made out of high heat conductivity fine grain graphite. In order to reduce its ohmic losses it has a copper coating on the reflecting surface. High power tests at the Max-Planck-Institut fuer Plasmaphysik, Greifswald, using a 750 kW beam at 140 GHz with repetitive pulses of 20 s proved the thermal stability of the metallic layer. Two different types of drives are used for the launcher. A slow drive rotates the launcher around its axis on a shot to shot basis, mainly to set the toroidal launching angle. A fast spindle drive controls the poloidal launching angle during a discharge. Fig. 12 shows the first two launchers built into ASDEX Upgrade. Fig. 13 plots the result of a dynamical test of the launcher during a typical ASDEX Upgrade plasma discharge. The launcher movement (solid line) contains both acceleration and deceleration of the mirror as well as a phase with constant velocity. There is also a delay in the response to the start and stop signal of the remote control (dashed line). The design value of $10^\circ / 100$ msec for the fast poloidal steering was achieved during the tests. Currently two more launchers are being built into the port. This capability will allow feedback control of the deposition on the time scale of NTM growth, providing the possibility to validate this scheme for ITER in ASDEX Upgrade.

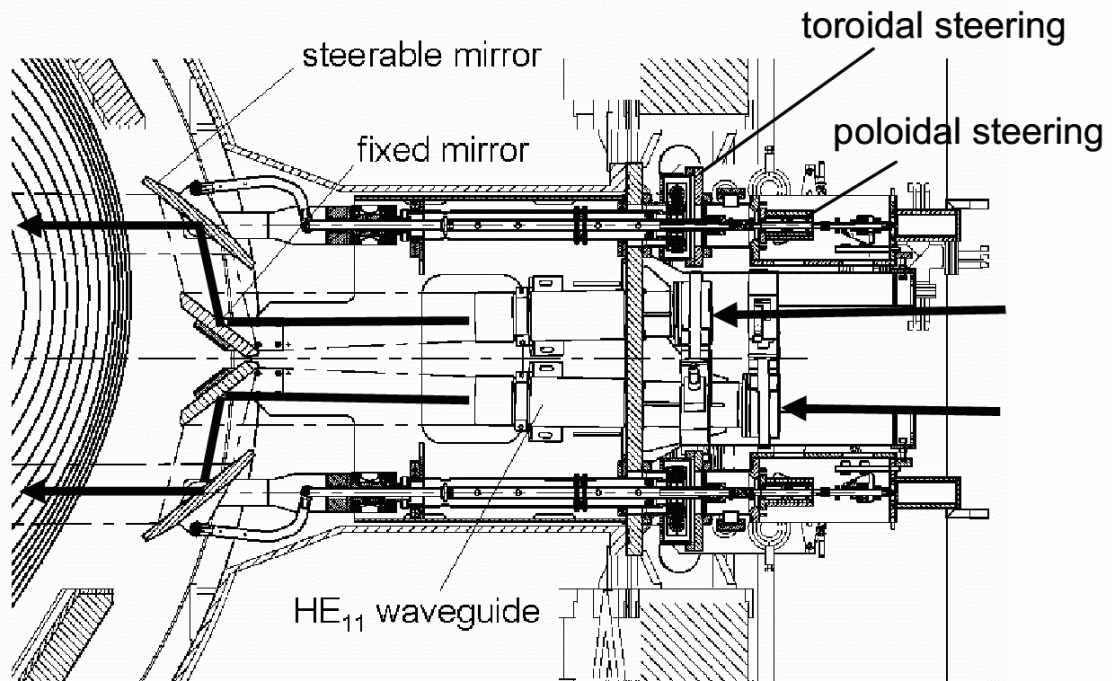


Fig. 11 ECRH launcher with a fast spindle drive for fast poloidal steering and a slow worm gear drive to set the toroidal angle.

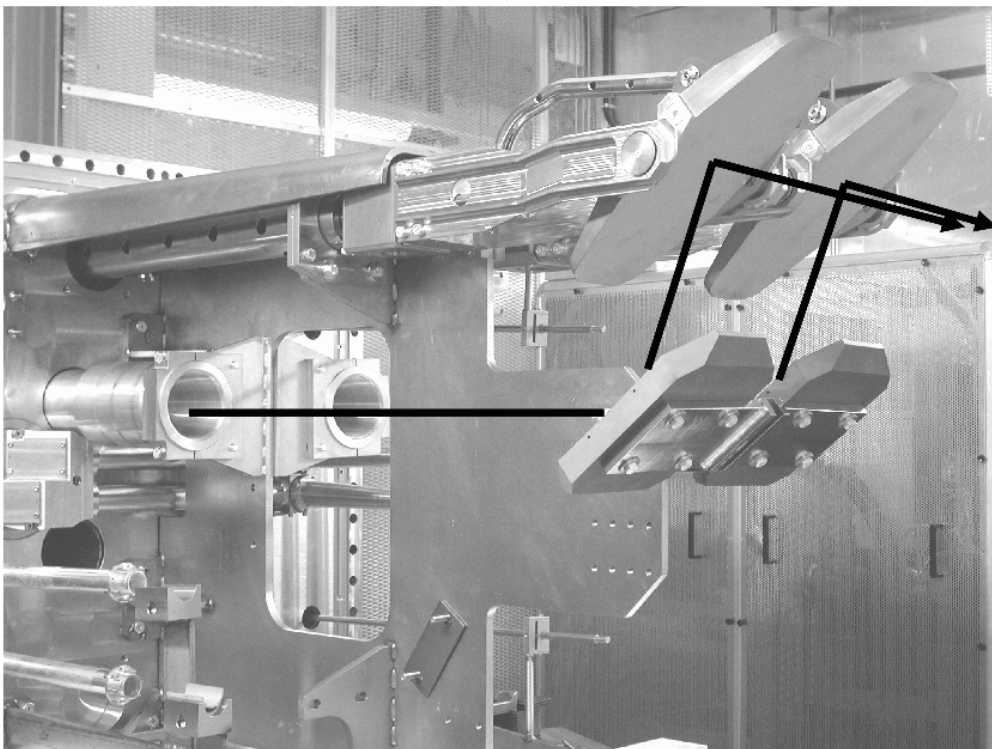


Fig. 12 First two launchers built into an ASDEX Upgrade port.

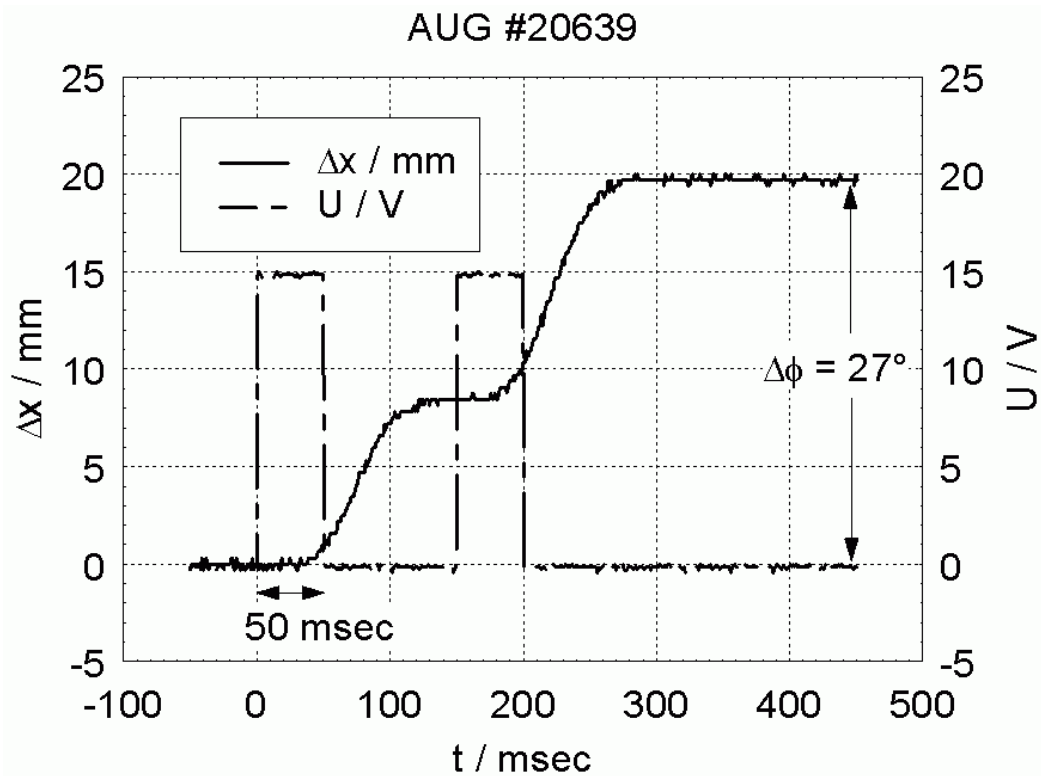


Fig. 13 Dynamical test of the fast steerable launcher during an ASDEX Upgrade shot.
Dashed line: control voltage, solid line: adjustable stroke of the fast spindle drive.

6. Conclusion

A multi-frequency ECRH system (4 MW, 10 s pulse length, frequency range 105-140 GHz) is currently under construction at the ASDEX Upgrade tokamak. This system poses new challenges not only to gyrotron development, but also to the matching optics and transmission elements, which have to be broadband. A first two-frequency gyrotron and transmission line of the new step-tunable ECRH system at ASDEX Upgrade have been successfully tested. Further extension to four gyrotrons and transmission lines is underway. A fast steerable launcher, which will be used for feedback controlled deposition, was tested under experimental conditions during plasma discharges in ASDEX Upgrade. The installation of broadband vacuum windows in the next gyrotrons and at the torus will allow for the operation at additional intermediate frequencies. With this system, the first large scale multi-frequency ECRH system on a fusion device will be realized, leading to unprecedented flexibility in ECRH operation on ASDEX Upgrade.

References

1. H. Zohm and M. Thumm, "On the use of step-tunable gyrotrons in ITER", *J. of Phys: Conf. Series*, **25**, 274-282, (2005).
2. F. Leuterer et al., "Plans for a new ECRH System at ASDEX Upgrade", *Fusion Eng. Des.*, **66-68**, 537-542, (2003).
3. K.E. Kreischer and R.J. Temkin, "High frequency gyrotrons and their application to tokamak plasma heating", *Int. J. on Infrared and Millimeter Waves*, **7**, 377-485, (1983).
4. M. Thumm, et al., "Frequency step-tunable (114–170 GHz) megawatt gyrotrons for plasma physics applications", *Fus. Eng. Des.* **53**, 407-421, (2001).
5. V. Zapevalov, et al., "Development of a Prototype of a 1-MW 105-156-GHz Multifrequency Gyrotron", *Radiophysics and Quantum Electronics* **47**, 396-404, (2004).
6. M. Maraschek et al., "Enhancement of the Stabilisation Efficiency of a Neoclassical Magnetic Island by Modulated Electron Cyclotron Current Drive in the ASDEX Upgrade Tokamak", submitted to *Physics Review Letters*, 2006.
7. P. Woskov et al., "Frequency Measurements of the Gyrotrons used for CTS Diagnostics at TEXTOR and ASDEX Upgrade", 16th APS High Temperature Plasma Diagnostics Conference, Williamsburg, VA, May 7-11, 2006.
8. G.I. Zaginaylov et al., "Influence of background plasma on electromagnetic properties of "cold" gyrotron cavity", *IEEE Trans. Plasma Sci.*, **34 (3)**, 512-517, (2006).
9. D. Wagner and F. Leuterer, "Broadband Polarizers for High-Power Multi-Frequency ECRH Systems", *Int. J. on Infrared and Millimeter Waves*, **26**, 163-172, (2005).